RUHR-UNIVERSITÄT BOCHUM

RUB

CR propagation and magnetic fields in galactic halos: observational evidence of CR driven galactic winds ?

Ralf-Jürgen Dettmar, Ruhr-University Bochum

with V. Heesen, B. Adebahr, R. Beck, M. Krause,Y. Stein, M. Wezgowiec, A. Miskolczi, George Heald and the LOFAR MKSP & CHANGES teams

RUHR-UNIVERSITÄT BOCHUM

RUB

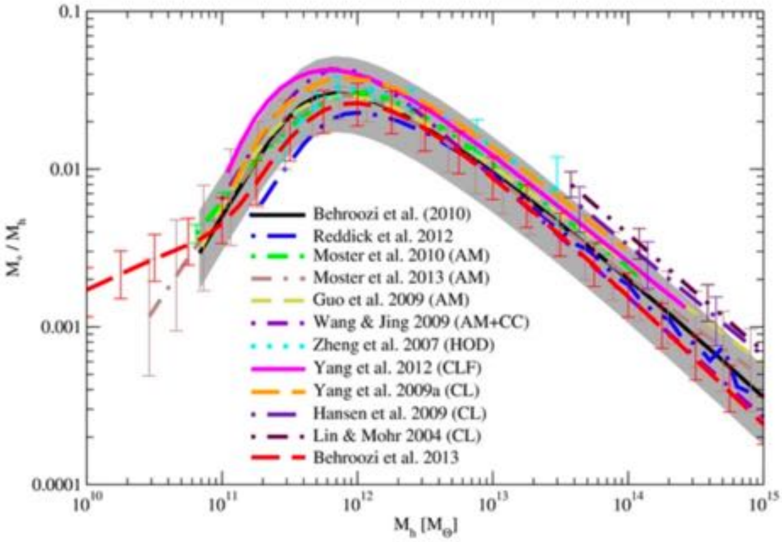

Behroozi+ 2013

RUHR-UNIVERSITÄT BOCHUM

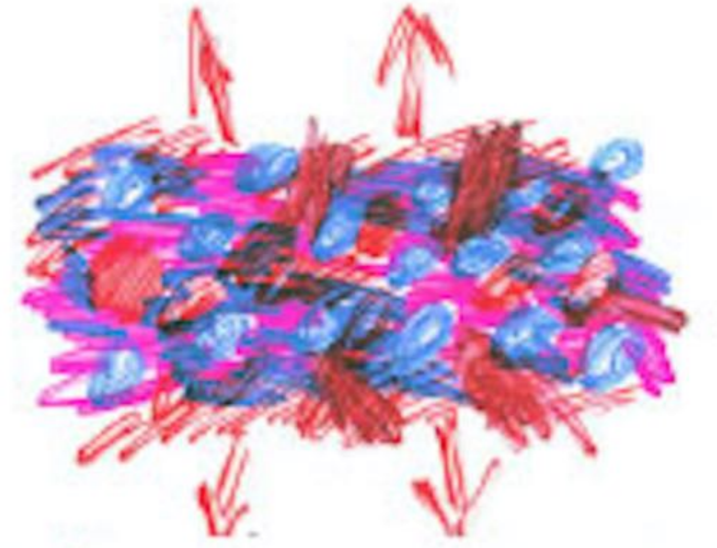

Silk 2013

Processes in the interstellar medium

(from Taylor, Cambridge Univ. Press)

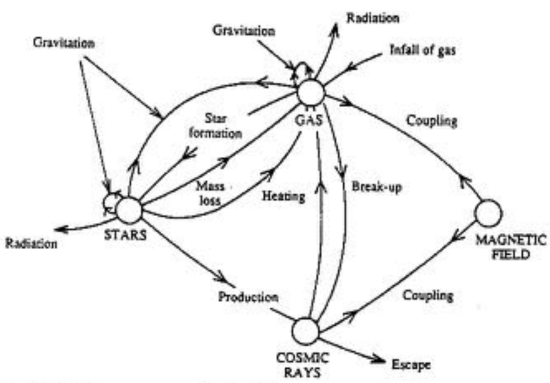

Magnetic Fields and Cosmic Rays contribute significantly to the energy density:

$U_{rad} \sim U_{\boldsymbol{B}} \sim U_{CR} \sim U_{kin}$

Cosmic ray-driven winds

LAUNCHING COSMIC-RAY-DRIVEN OUTFLOWS FROM THE MAGNETIZED INTERSTELLAR MEDIUM

Philipp Girichidis[1], Thorsten Naab[1], Stefanie Walch[2], Michał Hanasz[3], Mordecai-Mark Mac Low[4,5], Jeremiah P. Ostriker[6], Andrea Gatto[1], Thomas Peters[1], Richard Wünsch[7], Simon C. O. Glover[5], Ralf S. Klessen[5], Paul C. Clark[8], and Christian Baczynski[5] —Hide full author list

Published 2016 January 6 • © 2016. The American Astronomical Society. All rights reserved.
The Astrophysical Journal Letters, Volume 816, Number 2

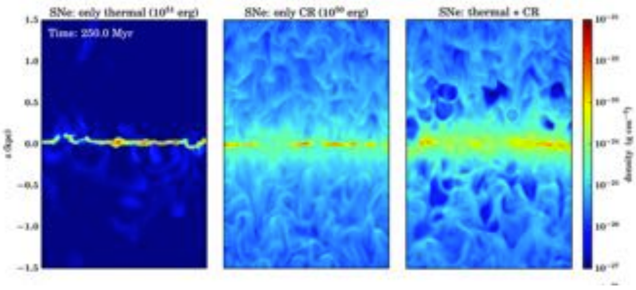

Salem & Bryan (2014)

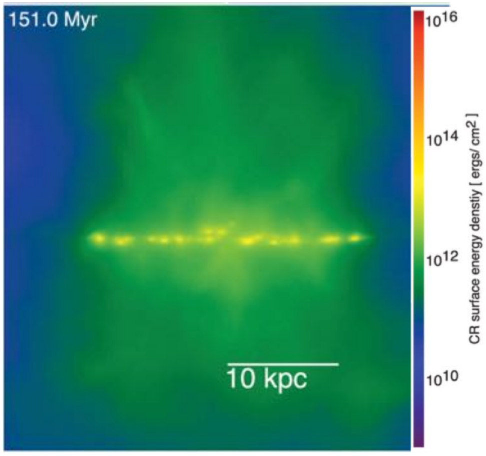

RUHR-UNIVERSITÄT BOCHUM

ApJ 777, L16 (2013)

SIMULATIONS OF DISK GALAXIES WITH COSMIC RAY DRIVEN GALACTIC WINDS

C. M. Booth[1], Oscar Agertz[2,1], Andrey V. Kravtsov[1,3,4], and Nickolay Y. Gnedin[5,1,3]

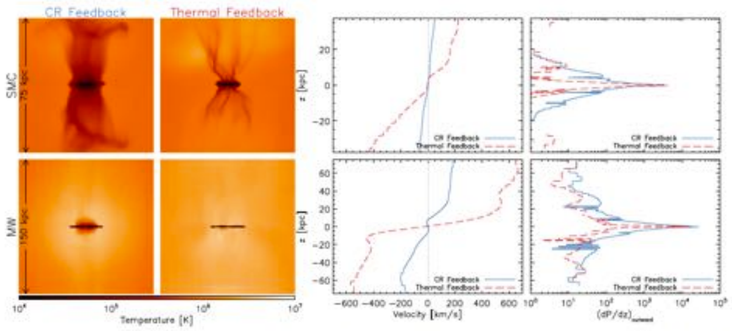

Fig. 3.— Edge-on maps of the temperature in a thin slice around the MW (*top panels*) and SMC galaxies (*bottom panels*) for both the thermal feedback *left panels*) and CR feedback (*right panels*). CR feedback has a large effect on the temperature structure of the halo gas. The plots show the median velocity (*left panels*) and outward pressure force (*right panels*) as a function of height from the disk for the same two simulations. All quantities are calculated in a cylinder of radius 3kpc, centered on the galactic disk. It is clear that the effect of the CRs is to increase the outward pressure forces in the halo by a factor of 3-5 at all z. This pressure gradient slowly accelerates the wind into the halo. The wind in the thermal feedback simulations is accelerated abruptly from the disk and maintains a constant velocity thereafter.

What we can measure: synchrotron emission from CR electrons

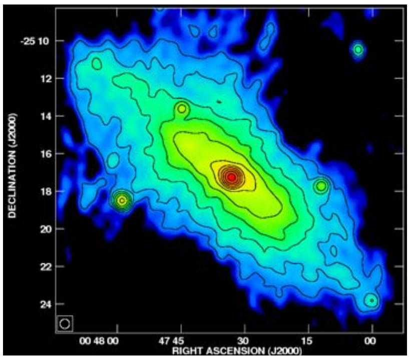

NGC 253 radiocontinuum study at 3, 6, 20, 90 cm

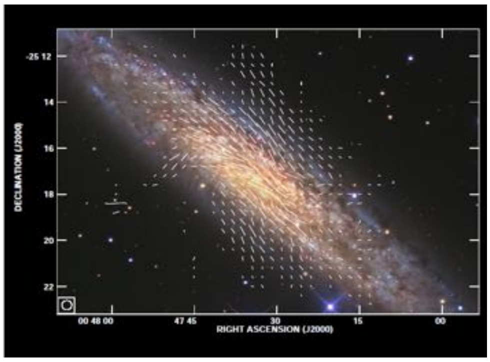

(Heesen, Krause, Beck, Dettmar 2009 A&A)

Polarized emission (and angles):

$I \propto \int n_{CR} B_{\perp}^{1+\alpha}\, dl$

Faraday rotation measures of the diffuse polarized emission:

$RM \propto \int n_e B_{\parallel}\, dl$

example LOFAR: LoTSS survey

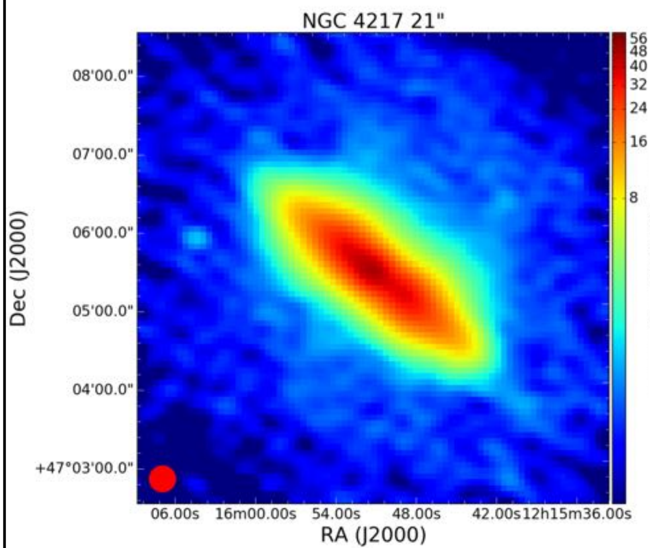

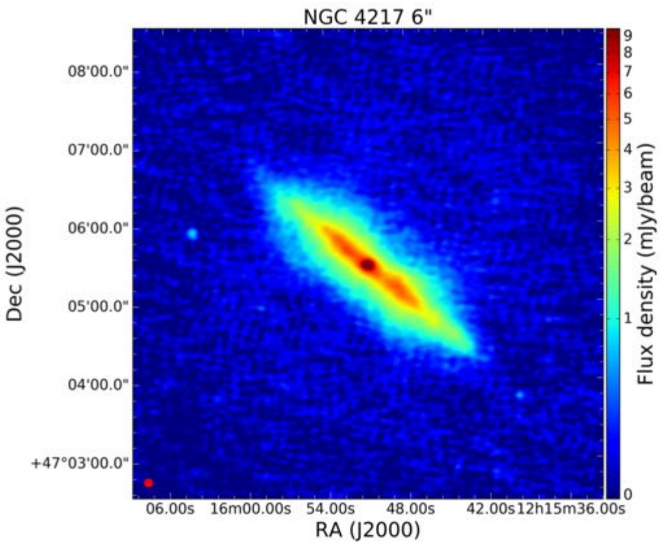

~0.1 mJy rms noise, 0.46Jy total flux (A. Miskolczi)

Ooty Synthesis Radio Telescope 143

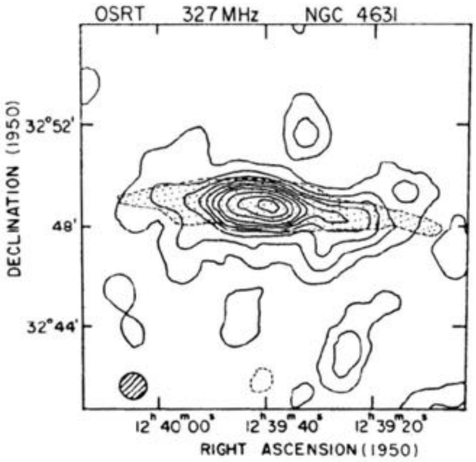

Figure-2. A327-MHz map of NGC 4631 made with a 60-arcsec Gaussian beam. The contour levels are – 15,15,45,75,105,135,165,195,245,295 and 345 mJy/beam. The optical image of the galaxy is marked by a broken line and is shaded by dots.

G. Swarup (1984)

auxiliary data:
thermal/non-thermal separation

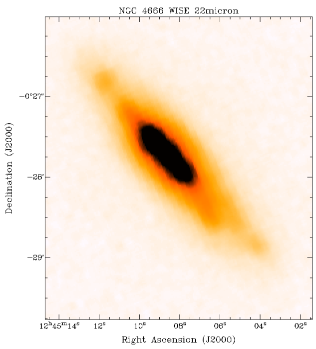

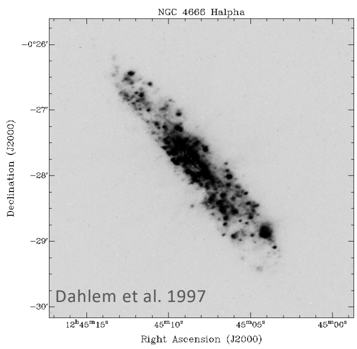

Dust corrected Hα image as thermal emission:

- WISE (22 μm) and Hα (in erg/s)
- Smoothing, regridding
- Calculating thermal Flux based on Calzetti et al. 2007

$F_{thermal} = C \ (L_{H\alpha} + 0.04\ L_{WISE})$

C. Vargas+ 2018. CHANG-ES X: Spatially Resolved Separation of Thermal Contribution from Radio Continuum Emission in Edge-on Galaxies

"clean non-thermal emission": 1D Modelling of CR–Transport

N(E, z): Cosmic Ray Electron number (column) density

Advection: $$\frac{\partial N(E,z)}{\partial z} = \frac{1}{V}\left\{\frac{\partial}{\partial E}[b(E)N(E,z)]\right\}$$

Diffusion: $$\frac{\partial^2 N(E,z)}{\partial z^2} = \frac{1}{D}\left\{\frac{\partial}{\partial E}[b(E)N(E,z)]\right\}$$

CRe losses: $$-\left(\frac{\mathrm{d}E}{\mathrm{d}t}\right) = b(E) = \frac{4}{3}\sigma_{\mathrm{T}}c\left(\frac{E}{m_{\mathrm{e}}c^2}\right)^2(U_{\mathrm{rad}} + U_{\mathrm{B}})$$

iC losses (U_{rad})

synchrotron radiation (U_{B})

CRE transport: SPINNAKER (V. Heesen)

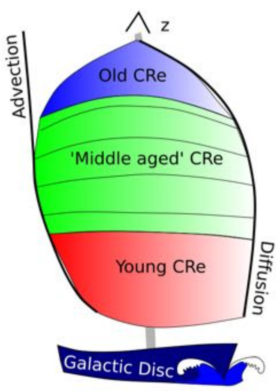

- **Sp**ectral **In**dex **N**umerical **A**nalysis of **K**(c)osmic-ray **E**lectron **R**adio-emission
- www.github.com/vheesen/Spinnaker

Advection models

h_B = 4 kpc h_B = 8 kpc h_B = 1e4 kpc

N(E,z)

$I_{nt}(z)$

α_{nt}

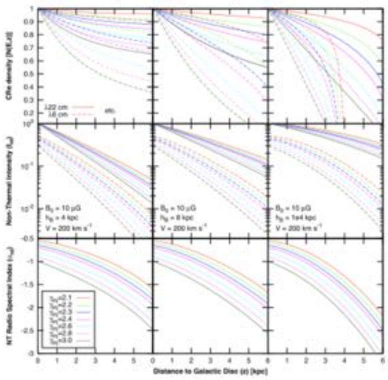

Diffusion models

h_B = 4 kpc h_B = 8 kpc h_B = 1e4 kpc

N(E,z)

$I_{nt}(z)$

α_{nt}

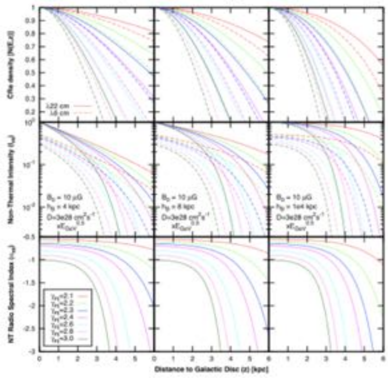

(V. Heesen)

Example: ATCA Observations

22 + 6 cm, radio continuum polarimetry

~160 hr at 22 cm and ~60 hr at 6 cm each

rms: ~30 μJy/beam at 22 cm and ~15 μJy/beam at 6 cm

Cleaned with CASA multi-scale CLEAN

N7090

N7462

analysis of CR transport (ATCA 6&20cm)

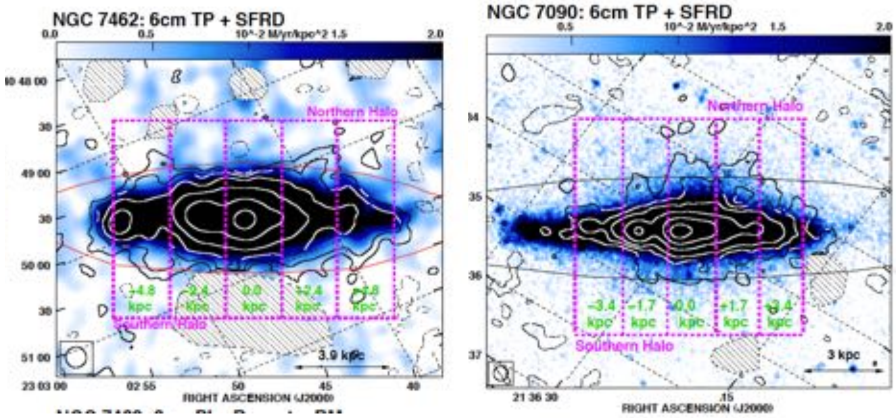

Heesen+ 2016 MNRAS 458, 332

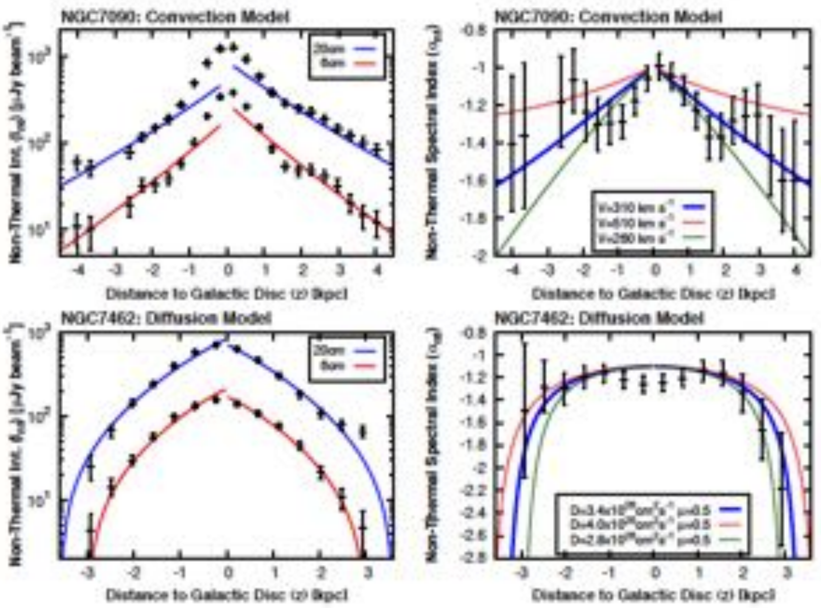

Table 2. Observation details for the galaxies presented in this paper.

Galaxy	Band[a]	ν^b (GHz)	Telescope[c]	Configuration[d]	Project[e]	Time[f] (h)	Date[g]	Notes[h]	Reference[i]
NGC 55	*L*	1.37	ATCA	750D	C287	8.7	1993 Aug 1	Mosaic	17
...	...	...	...	375	C287	11.2	1995 Jan 12	...	...
...	...	...	...	750A	C287	11.1	1995 Oct 25	...	...
...	...	...	...	H75	C1341	5.0	2005 Jul 17	Mosaic	This work
...	...	...	...	EW352	C1341	9.4	2005 Oct 7	...	...
...	*C*	4.80	...	375	C287	3.6	1994 Mar 29	Mosaic	17
...	...	...	...	375	C287	10.2	1994 Mar 30	...	...
...	...	...	...	375	C287	7.8	1994 Mar 31	...	...
...	...	...	...	375	C287	12.5	1994 Nov 23	...	...
...	...	...	...	750A	C287	5.1	1995 Mar 1	...	...
...	...	...	...	375	C287	5.3	1995 Aug 16	...	...
...	...	...	...	375	C287	10.2	1995 Nov 24	...	...
...	...	4.67	...	EW352	C1974	7.6	2008 Nov 22	...	This work
...	...	...	...	EW364	C1974	9.9	2009 Feb 13	...	...
...	*C*	5.60	...	H168	C1974	7.6	2010 Mar 27	...	...
...	*C*	4.80	Parkes	single-dish	P697	16.0	2010 Oct 7	Merged	...
NGC 253	*L*	1.46	VLA	B+C+D	AC278	4.1	1990 Sep–1991 Mar	Mosaic	2
...	*C*	4.86	...	D	AH844	35.8	2004 Jul 4–24	Mosaic	10
...	...	4.85	Effelsberg	single-dish	N/A	N/A	1997	Merged	...
NGC 891	*L*	1.39	WSRT	Multiple	R02B	240	2002 Aug–Dec		13
...	*C*	4.86	VLA	D	AA94	11.2	1988 Aug 29		16
...	...	4.85	Effelsberg	single-dish	44–95	9.1	1996 Feb–Aug		6
NGC 3044	*L*	1.49	VLA	B	AI28	3.1	1986 Aug 1		This work
...	...	...	...	C	AI23	0.8	1985 Jul 25		11
...	...	...	...	D	AI31	1.1	1987 Apr 28/30		...
...	*C*	4.86	...	C	AB676	0.8	1993 Jun 13		4
...	...	...	...	D	AM573	1.1	1997 Nov 6		This work
...	...	...	...	D	AI31	1.0	1987 Apr 28		11
NGC 3079	*L*	1.66	VLA	B	BS44	1.0	1997 Mar 8		This work
...	...	1.41	...	CD	BS44	2.4	1997 Oct 2		...
...	...	1.43	...	C	AB740	1.3	1996 Feb 17		...
...	*C*	4.71	...	C	AC277	3.9	1990 Dec 9		3
...	...	4.86	...	D	AD177	2.5	1986 Jan 16		This work
NGC 3628	*L*	1.49	VLA	CD	AS300	4.3	1988 Mar 25		14
...	...	...	...	D	AS300	8.4	1987 Apr 7		...
...	*C*	4.86	...	D	AK243	7.7	1991 Mar 28		7
NGC 4565	*L*	1.49	VLA	B	AS326	3.8	1988 Jan 29		16
...	...	1.48	...	D	AS326	10.6	1988 Aug 28		...
...	*C*	4.86	...	D	AK424	3.4	1996 Sep 28		6
NGC 4631	*L*	1.37	WSRT	maxi-short	N/A	6.0	2003 Apr 3		1
...	*C*	4.86	VLA	D	AH369	12.1	1989 Nov 22/26	Mosaic	9
...	...	...	...	D	AD896	4.3	1999 Apr 14	Mosaic	12
...	...	4.85	Effelsberg	single-dish	55–94	6.3	1996 Feb–Aug	Merged	6
NGC 4666	*L*	1.43	VLA	CD	AD346	3.5	1994 Nov 20		5
...	...	1.49	...	D	AS199	0.2	1984 Aug 31		This work
...	*C*	4.86	...	D	AD326	12.5	1993 Dec 20/24		5
NGC 5775	*L*	1.49	VLA	B	AI0028	3.2	1986 Aug 1		8
...	...	1.48	...	B	AB492	1.2	1989 Aug 4		...
...	...	1.49	...	C	AH368	3.6	1990 Nov 19/24		...
...	...	...	...	D	AI31	1.9	1987 Apr 27/30		11
...	*X*	8.45	...	D	AD455	13.4	2001 Dec 14		15

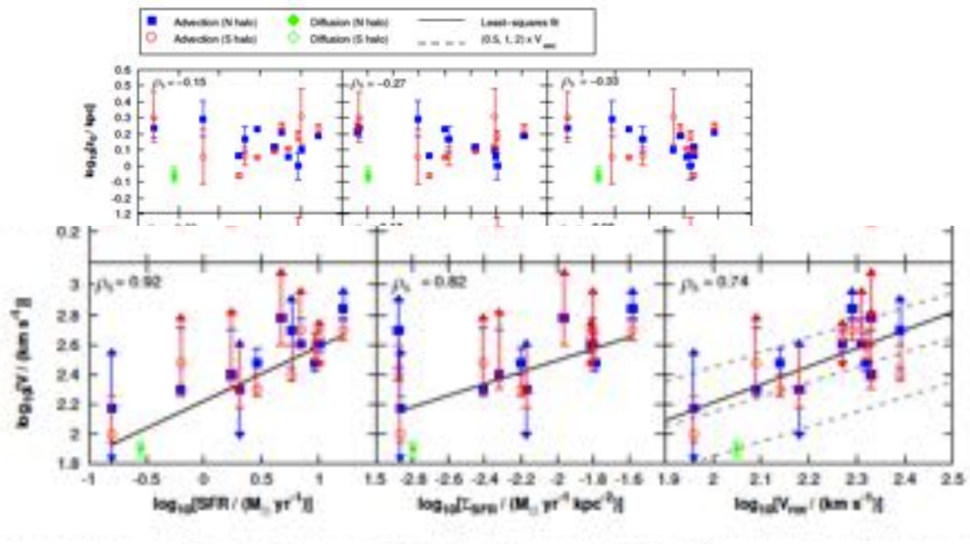

Figure 8. Parameter studies in log-log diagrams as function of SFR, SFR surface density (Σ_{SFR}) and rotation speed V_{rot}. *Top panels:* non-thermal intensity scale height at 5 GHz (8.5 GHz for NGC 5775) of the thick radio disc. *Middle panels:* magnetic field scale height of the thick radio disc. *Bottom panels:* Advection speed (V), where solid lines show least-squares fits. In the bottom right panel the dashed lines show $(0.5, 1, 2) \times V_{\mathrm{esc}}$. In each panel, we also present Spearman's rank correlation coefficient, ρ_s, which we derived from values that have both an upper and lower limits.

:

Heesen+ MNRAS 476,158 (2018)

CRAV (identical to NOCR but 10% of the SN energy in CR energy. The remaining 90% is added as thermal energy. The CR energy can advect with the gas

CRAD is identical to CRAV, but with *anisotropic* instead of isotropic CR diffusion (Pakmor et al. 2016a). The diffusion coefficient in this model is $\kappa = 10^{28}\,\mathrm{cm}^2\,\mathrm{s}^{-1}$ parallel to the magnetic field and zero in all transverse directions.

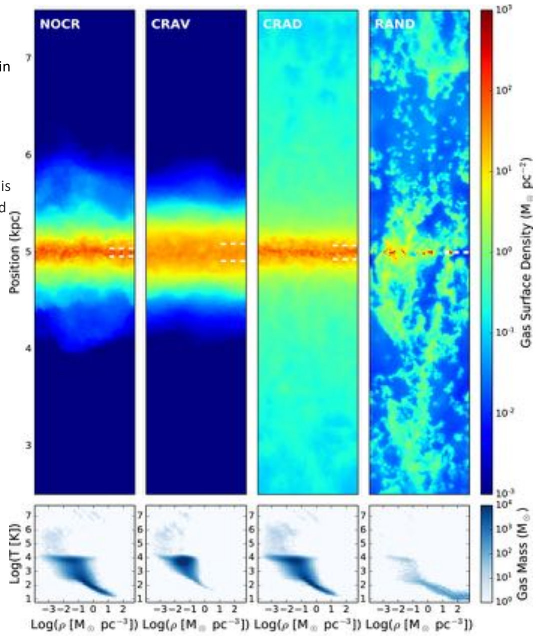

Christine M. Simpson et al. 2016 ApJL 827 L29

LOTSS 20“ **NGC4013** SDSS

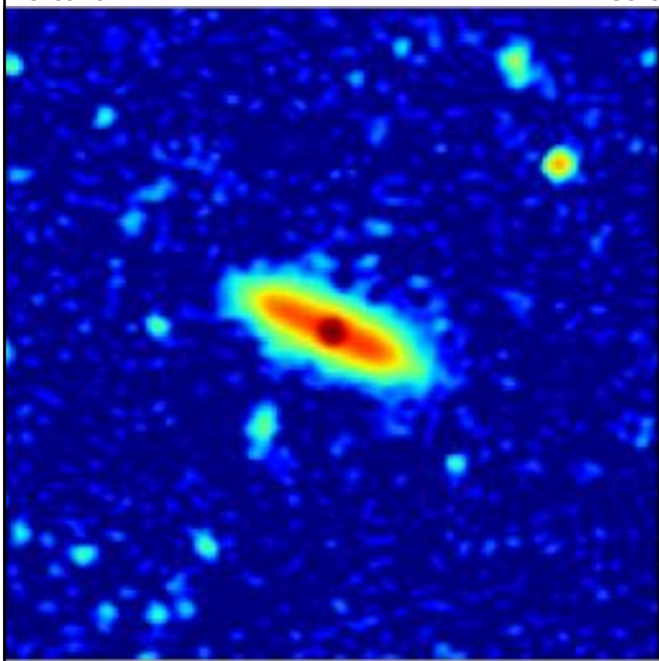

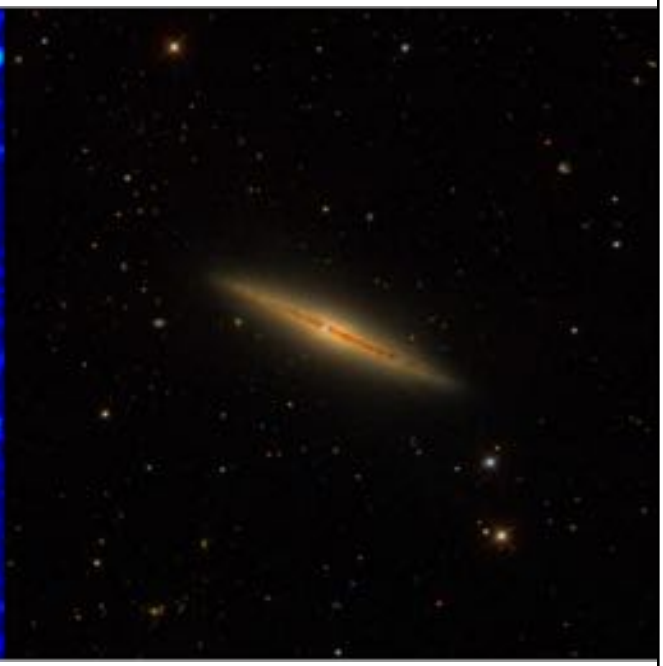

(A. Miskolczi)

LOFAR/LoTSS + JVLA

CHANGES:
Continuum HAlos in Nearby Galaxies
- an Evla Survey

PI: Judith Irwin, Kingston (ONT/CANADA)

35 edge-on galaxies

inclination > 75 deg
DEC > 25 deg
4 arcmin > D < 15 arcmin
flux > 23 mJy

+ a few well studied larger object

Large proposal 405 hours granted (RSRO)

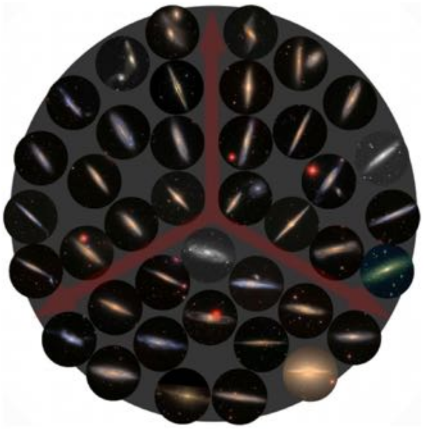

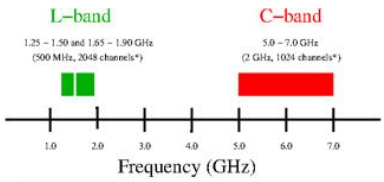

NGC 4013 LOTSS/JVLA C-Band

(Y. Stein+, 2019, submitted)

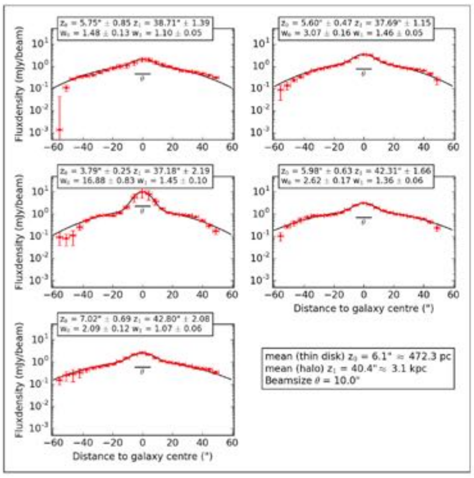

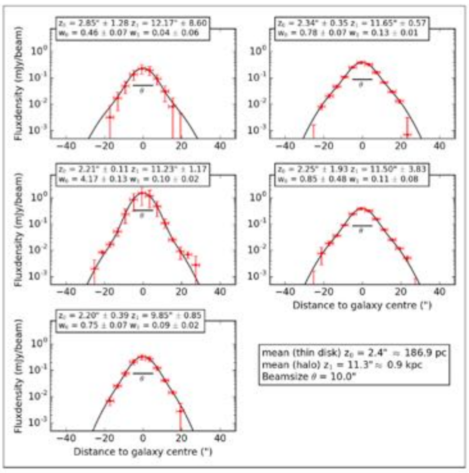

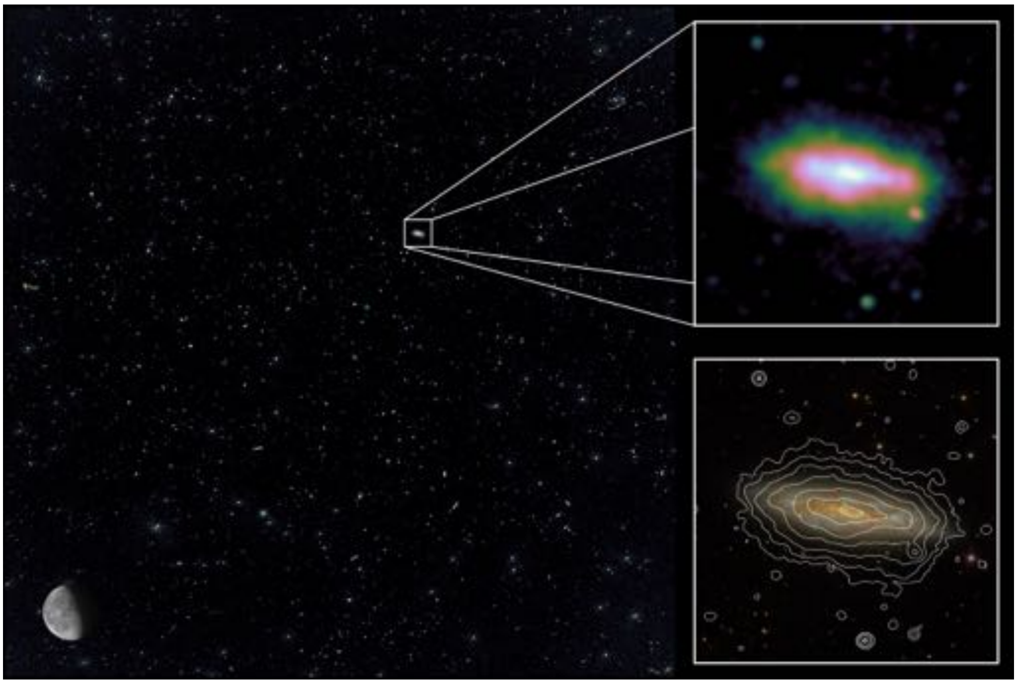

LOTSS NGC3556
(A. Miskolczi)

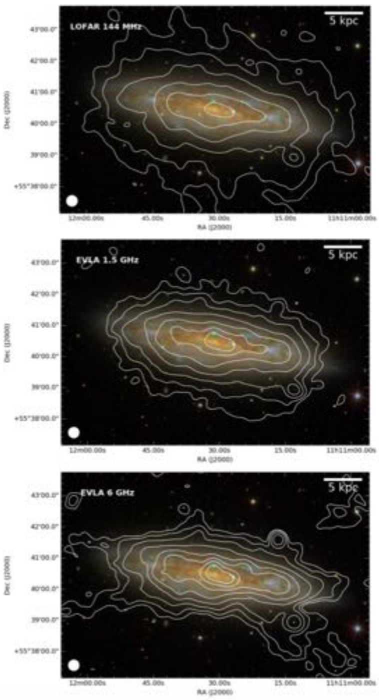

CHANGES XII: N3556 (Miskolczi+, 2019)

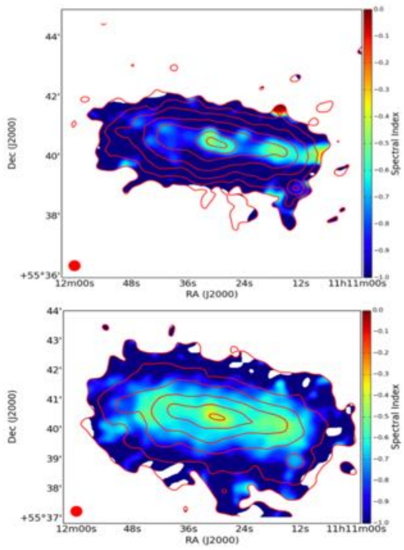

spectral index much better described using a wind profile for v

$$v(z) = v_0 \left(1 + \left(\frac{z}{h_{\rm v}}\right)^{\beta}\right).$$

LOFAR HBA 10hrs 118-192 MHz (Heald, Shridar, Heesen + LOFAR MKSP, in prep)

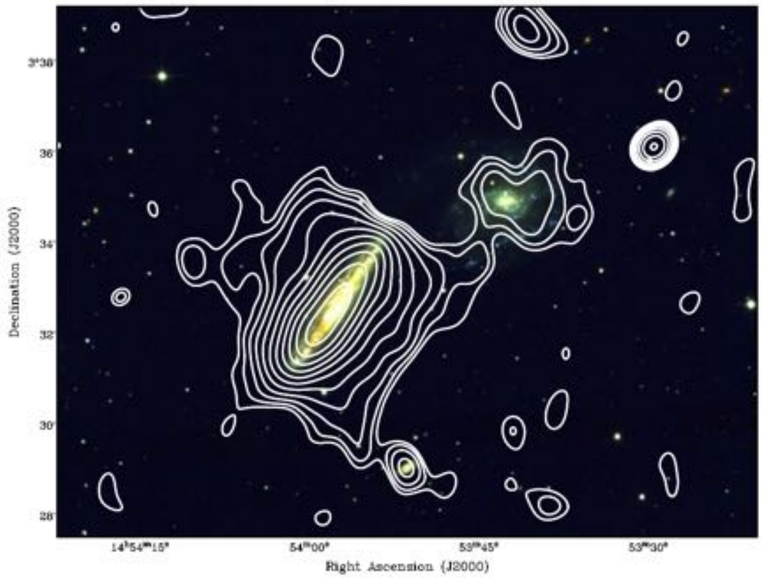

R.-J. Dettmar | CR driven galactic winds| MWSKY-II Pune

RUHR-UNIVERSITÄT BOCHUM

RUB

Summary:

- CRE transport seems to be dominated by advection in most star forming disk galaxies
- LOFAR observations allow us to study the low energy and „old“ population of CREs
- Surveys aiming at measurements of magnetic fields and CRs in halos of a larger number of objects are underway

Supported by BMBF „Verbundforschung bodengebundene Astronomie und Astrophysik“

Thank you

NGC 46666 Credit: Y. Stein, J. Englisch, A. Miskolczi